

This discussion paper is/has been under review for the journal Biogeosciences (BG).
Please refer to the corresponding final paper in BG if available.

Diurnal variation in the coupling of photosynthetic electron transport and carbon fixation in iron-limited phytoplankton in the NE subarctic Pacific

N. Schuback¹, M. Flecken², M. T. Maldonado¹, and P. D. Tortell^{1,3}

¹Departement of Earth, Ocean and Atmospheric Sciences, University of British Columbia, Vancouver, BC, Canada

²RWTH Aachen University, Aachen, Germany

³Department of Botany, University of British Columbia, Vancouver, BC, Canada

Received: 30 September 2015 – Accepted: 1 October 2015 – Published: 19 October 2015

Correspondence to: N. Schuback (nschuback@eos.ubc.ca)

Published by Copernicus Publications on behalf of the European Geosciences Union.

Diurnal variation in the coupling of photosynthetic electron transport

N. Schuback et al.

Title Page

Abstract

Introduction

Conclusions

References

Tables

Figures

⏪

⏩

◀

▶

Back

Close

Full Screen / Esc

Printer-friendly Version

Interactive Discussion



Abstract

Active chlorophyll *a* fluorescence approaches, including fast repetition rate fluorometry (FRRF), have the potential to provide estimates of phytoplankton primary productivity at unprecedented spatial and temporal resolution. FRRF-derived productivity rates are based on estimates of charge separation at PSII (ETR_{RCII}), which must be converted into ecologically relevant units of carbon fixation. Understanding sources of variability in the coupling of ETR_{RCII} and carbon fixation provides physiological insight into phytoplankton photosynthesis, and is critical for the application of FRRF as a primary productivity measurement tool. In the present study, we simultaneously measured phytoplankton carbon fixation and ETR_{RCII} in the iron-limited NE subarctic Pacific, over the course of a diurnal cycle. We show that rates of ETR_{RCII} are closely tied to the diurnal cycle in light availability, whereas rates of carbon fixation appear to be influenced by endogenous changes in metabolic energy allocation under iron-limited conditions. Unsynchronized diurnal oscillations of the two rates led to 3.5 fold changes in the conversion factor coupling ETR_{RCII} and carbon fixation ($\Phi_{e:C}/n_{PSII}$). Consequently, diurnal variability in phytoplankton carbon fixation cannot be adequately captured with FRRF approaches if a constant conversion factor is applied. Utilizing several auxiliary photophysiological measurements, we observed that a high conversion factor is associated with conditions of excess light, and correlates with the expression of non-photochemical quenching (NPQ) in the pigment antenna, as derived from FRRF measurements. The observed correlation between NPQ and the conversion factor $\Phi_{e:C}/n_{PSII}$ has the potential to improve estimates of phytoplankton carbon fixation rates from FRRF measurements alone.

Diurnal variation in the coupling of photosynthetic electron transport

N. Schuback et al.

Title Page

Abstract

Introduction

Conclusions

References

Tables

Figures



Back

Close

Full Screen / Esc

Printer-friendly Version

Interactive Discussion



1 Introduction

Marine phytoplankton account for $\sim 50\%$ of global carbon fixation (Field et al., 1998), and play a key role in Earth's biogeochemical cycles. Understanding the spatial and temporal patterns in marine primary productivity and its response to environmental variability is thus a central oceanographic research question. Traditionally, rates of phytoplankton primary production have been measured using incubation-based assays, tracing the evolution of oxygen or the assimilation of CO_2 (Williams et al., 2008). More recently, bio-optical approaches based on measurements of active chlorophyll *a* fluorescence (ChlF) yields (Kolber and Falkowski, 1993; Schreiber, 2004) have emerged as an attractive alternative, avoiding artifacts related to bottle containment, and achieving unparalleled spatial and temporal resolution. The method most prominently applied to measure ChlF yields in field assemblages of marine phytoplankton is fast repetition rate fluorometry (FRRF) (Kolber et al., 1998). ChlF yields, as measured by FRRF, can be used to estimate electron transport in photosystem II (ETR_{RCII} , $\text{mol e}^- \text{mol RCII}^{-1} \text{s}^{-1}$), and these rates can be converted to carbon units based on theoretical calculations. However, empirical comparison of FRRF-derived ETR_{RCII} and carbon fixation data has shown that the derived conversion factor varies significantly with changes in the physiology and taxonomic composition of phytoplankton assemblages (Suggett et al., 2010; Lawrenz et al., 2013).

The conversion factor linking ETR_{RCII} and carbon fixation consists of two parameters, the amount of chlorophyll *a* per number of functional PSII reaction centers ($1/n_{\text{PSII}}$; $\text{mol chl } a \text{ mol RCII}^{-1}$) and the electron requirement for carbon fixation ($\Phi_{\text{e,C}}$; $\text{mol e}^- \text{mol C}^{-1}$). Plasticity in both parameters can be observed at the physiological and taxonomic level, and is ultimately a function of given environmental conditions. Marine phytoplankton evolved to optimize growth under fluctuating light and often limiting nutrient conditions. As a consequence, phytoplankton photosynthesis and downstream metabolic processes exhibit great plasticity and interconnectivity, allowing rapid responds to changes in environmental conditions. This physiological regulation influ-

BGD

12, 16803–16845, 2015

Diurnal variation in the coupling of photosynthetic electron transport

N. Schuback et al.

Title Page

Abstract

Introduction

Conclusions

References

Tables

Figures

◀

▶

◀

▶

Back

Close

Full Screen / Esc

Printer-friendly Version

Interactive Discussion



Diurnal variation in the coupling of photosynthetic electron transport

N. Schuback et al.

Title Page

Abstract

Introduction

Conclusions

References

Tables

Figures

⏪

⏩

◀

▶

Back

Close

Full Screen / Esc

Printer-friendly Version

Interactive Discussion



5
10
15
20
25

mary productivity from FRRF measurements, and should be considered, along with phytoplankton taxonomy and nutrient status (Lawrenz et al., 2013), when deriving regional conversion factors between ETR_{RCII} and carbon fixation. Building on previously published results (Schuback et al., 2015), we show that the magnitude and variability of $\Phi_{e:C}/\eta_{PSII}$ can be correlated to FRRF-based measurements of non-photochemical quenching (NPQ_{NSV}).

2 Methods

2.1 Study site and water-column hydrography

Field sampling was conducted on board the CCGS *John P. Tully* on 17/18 June 2014. During the sampling period, the research vessel stayed within close proximity (10 km) to Ocean Station Papa (OSP), located in iron-limited waters of the NE subarctic Pacific (50° N, 145° W) (<https://www.waterproperties.ca/linep/>). We acknowledge that our sampling approach is not truly Lagrangian, and some variability in nutritional status and taxonomic composition of phytoplankton assemblage could have occurred due to water mass advection. However, we expect that surface hydrography and phytoplankton characteristics are sufficiently homogeneous in this oceanic region, such that minor water mass advection would not have significantly influenced primary productivity or photophysiological parameters measured over the diurnal cycle.

During our occupation of OSP, we conducted five CTD casts (three casts during the 24 h diurnal experiment and one each before and after the diurnal sampling) to characterize variability in temperature and salinity depth profiles, from which we derived sea-water density using the GSW toolbox in MATLAB (McDougall and Barker, 2011). Mixed layer depth (MLD) was calculated from a density difference criterion ($\Delta\sigma = 0.05$). The depth profile of photosynthetically available radiation (PAR, 400–700 nm, $\mu\text{mol quanta m}^{-2} \text{s}^{-1}$) through the upper 100 m of the water column was obtained using a PAR sensor (Biospherical QSP-400) mounted on the rosette during one of the CTD casts

(12:30 local time, LT). The optical extinction coefficient, k_d (m^{-1}), was calculated as:

$$k_d = (\ln E_0 - \ln E_z)/z \quad (1)$$

where E_0 is surface irradiance and E_z is irradiance at depth z (m). Surface PAR (E_0^+) was continuously logged (10 min intervals) with a LI-1000 down-welling PAR sensor (LI-COR, USA), mounted in a non-shaded position on the ship's superstructure, at a height of ca. 7 m above the sea-surface. Unfortunately, 3 h of PAR data were lost due to an instrument malfunction. To fill the data gap, we utilized shortwave solar radiation data from a nearby moored surface buoy, operated by the Ocean Climate Stations (OCS) group at Pacific Marine Environmental Laboratory of the National Oceanic and Atmospheric Administration (PMEL-NOAA). All mooring data are available from the NOAA OCS website (<http://www.pmel.noaa.gov/OCS>). We aligned the two sets of irradiance data (ship-based and surface mooring) and extrapolated over the 3 h gap in order to obtain consistent E_0^+ for the timespan of the diurnal experiment. Surface reflectance was calculated as a function of solar zenith angle following Kirk (2011) using the R package "phytotools" (Silsbe, 2015). Subtracting surface reflectance provides PAR just under the air-ocean interface (E_0^-). PAR at 5 m depth ($E_{5\text{m}}^-$) was calculated as $E_{5\text{m}}^- = E_0^- \exp(k_d \times 5\text{m})$.

Macro-nutrients (P, N, Si) were measured on samples from 2 CTD-rosette casts following the methods outlined in Barwell-Clarke (1996). Additional measurements of surface water (~ 5 m) temperature and salinity were derived from the ship's thermosalinograph (TSG) connected to a continuous seawater supply, and also from the NOAA mooring.

2.2 Sample collection

Seawater samples were collected from the seawater intake system (ca. 5 m depth) every 3 h over a 24 h period and processed immediately for a variety of physiological assays described below. The resulting dataset consists of 8 time-points (TPs). Local

16808

Diurnal variation in the coupling of photosynthetic electron transport

N. Schuback et al.

Title Page

Abstract

Introduction

Conclusions

References

Tables

Figures

◀

▶

◀

▶

Back

Close

Full Screen / Esc

Printer-friendly Version

Interactive Discussion



sunrise, solar noon and sunset were at 6:30, 14:40 and 22:50 LT, respectively, resulting in 3 night-time TPs (3:00, 23:00, 0:00 LT) and 5 day-time TPs (6:00, 9:00, 12:00, 15:00, 18:00 LT). Samples taken at each TP are summarized in Table 1.

2.3 [chl *a*] and HPLC

At each TP, duplicate 500 mL samples for [chl *a*] were filtered onto pre-combusted 25 mm glass fiber filters (GF/F) using low vacuum pressure (< 5 mm Hg), taking care to keep the filters out of direct light. Filters were stored at -20°C and analyzed following the method of Welschmeyer (1994) within two weeks of collection. At 4 TPs (3:00, 9:00, 15:00, 21:00 LT) duplicate 2.2 L samples for pigment analysis were filtered onto pre-combusted 25 mm GF/F, as above. Filters were blotted dry with absorbent paper, flash frozen in liquid nitrogen and stored at -80°C until analysis by reverse-phase high pressure liquid chromatography (HPLC) following the method of (Pinckney, 2013). In order to assess diurnal changes in the extent of light stress experienced by the phytoplankton assemblage, we derived a number of pigment ratios (Table 2). We also used the pigment data to estimate the relative abundance of different phytoplankton taxa at our sampling site. CHEMTAX analysis was performed using the averaged pigment concentrations from each TP. Analysis was performed essentially as described in Taylor et al. (2013). The initial pigment ratio matrix, specific to North Pacific phytoplankton isolates, was taken from Table 5 in Lee et al. (2011).

2.4 Absorption spectra

Absorption spectra of phytoplankton cellular pigments ($a_{\text{phy}}(\lambda)$) were determined following the quantitative filter technique (QFT) as described in (Mitchell et al., 2002). At each TP, duplicate 1.1 L samples were filtered onto pre-combusted 25 mm GF/F under low vacuum pressure and light, taking care to achieve even sample distribution on the filter. Reference filters were prepared by filtering 1.1 L of Milli-Q water. Filters were carefully placed into 25 mm tissue capsules (Fisher), flash frozen in liquid nitrogen and stored at

BGD

12, 16803–16845, 2015

Diurnal variation in the coupling of photosynthetic electron transport

N. Schuback et al.

Title Page

Abstract

Introduction

Conclusions

References

Tables

Figures

◀

▶

◀

▶

Back

Close

Full Screen / Esc

Printer-friendly Version

Interactive Discussion



–80 °C until analysis within 1 month of the experiment. Sample filters were analyzed on a Cary BIO-100 dual-beam spectrophotometer (Varian) against reference filters as described in Mitchell et al. (2002). Optical density (OD) was measured from 370–800 nm (1 nm resolution) before and after extraction of pigment with 90 % methanol (Kishino et al., 1985) to determine OD of the whole particulate sample and OD of detritus after pigment extraction, respectively. Each sample and blank was analyzed in triplicate, to minimize error associated with instrument measurements. The wavelength-specific phytoplankton pigment absorption spectrum ($a_{\text{phy}}(\lambda), \text{m}^{-1}$) was calculated as:

$$a_{\text{phy}}(\lambda) = 2.303 \times (\text{OD}_{\text{sample}}(\lambda) - \text{OD}_{\text{detritus}}(\lambda)) \times \frac{A}{V} \times \beta^{-1} \quad (2)$$

where 2.303 is the conversion of from base-10 to a natural logarithm, A is the particulate retention area of the filter (m^2), V is the volume filtered (m^3), and β is the path-length amplification coefficient (4.5, Roettgers and Gehnke, 2012). To determine chl a specific absorption spectra ($a^*_{\text{phy}}(\lambda), \text{m}^{-1} \text{mg chl } a^{-1}$), values were normalized to corresponding [chl a] values. Absorption spectra were used for spectral correction of our rate measurements, as described in detail below.

2.5 FRRF-derived photophysiological parameters and ETR_{RCII}

All FRRF measurements were conducted on a bench top FRRF instrument (Soliense Inc.), as described in Schuback et al. (2015). Briefly, we applied a single turnover (ST) protocol (100 flashlets with 1.0 μs length and 2.5 μs interval, 46 200 μmol quanta $\text{m}^{-2} \text{s}^{-1}$ peak power intensity, resulting in a ST flash length of 250 μs , providing ~ 5–10 quanta per RCII), during which excitation power was provided by an array of eight LEDs at four wavelengths centered on 445, 470, 505, and 530 nm (equal intensity from each wavelength). We measured steady state light curves (SSLC), where each sample was exposed to 10 actinic “background” irradiances from 0 to 1000 μmol quanta $\text{m}^{-2} \text{s}^{-1}$, provided at the same four wavelengths. All ChlF yields and parameters described below were derived by an iterative non-linear fitting procedure, applying the

BGD

12, 16803–16845, 2015

Diurnal variation in the coupling of photosynthetic electron transport

N. Schuback et al.

Title Page

Abstract

Introduction

Conclusions

References

Tables

Figures

◀

▶

◀

▶

Back

Close

Full Screen / Esc

Printer-friendly Version

Interactive Discussion



Diurnal variation in the coupling of photosynthetic electron transport

N. Schuback et al.

Title Page

Abstract

Introduction

Conclusions

References

Tables

Figures



Back

Close

Full Screen / Esc

Printer-friendly Version

Interactive Discussion



four parameter biophysical model of Kolber et al. (1998) to a mean of 20 consecutive ST flashlet sequences using custom software (Z. Kolber). This software accounts for the formation of fluorescence quenching, most likely due to formation of a P680 triplet, which reduces the maximum fluorescence yield attainable during the ST flash by 3–6%. Throughout the SSLC, ST flashlet sequences were measured continuously (1 s interval) and the length of each light step was optimized to allow all derived parameters to reach steady state (ca. 3 min). ChlF yields and parameters corresponding to each light level were obtained from the mean of the last three acquisitions at each light level. In this way, we derived the fluorescence yields F_o and F_m (in dark-regulated state) as well as F'_o and F'_m (in the light regulated state for each light level of the SSLC). F'_o was calculated as $F'_o = F_o / (F_v / F_m + F_o / F'_m)$ (Oxborough and Baker, 1997).

The five fluorescence yields F_o , F_m , F'_o , F'_m and F'_o were used to calculate ChlF parameters, following (Roháček, 2002) as described in Schuback et al. (2015). Furthermore, the functional absorption cross section of PSII, $\sigma_{\text{PSII}} (\times 10^{-20} \text{ m}^2 \text{ RCII}^{-1})$, was derived from the rate of closure of RCII in the dark-regulated and each light-regulated state (Kolber and Falkowski, 1993; Kolber et al., 1998). We calculated ETR_{RCII} as:

$$\text{ETR}_{\text{RCII}} = E \times \sigma'_{\text{PSII}} \times F'_q / F'_v \times 0.006022 \quad (3)$$

where $E (\mu\text{mol quanta m}^{-2} \text{ s}^{-1})$ is the actinic irradiance at each light level, $\sigma'_{\text{PSII}} (\times 10^{-20} \text{ m}^2 \text{ RCII}^{-1})$ is the functional absorption cross section of PSII at each light level, and $F'_q / F'_v (= qP)$ is the quantum efficiency of photochemical energy conversion in RCII at a given light intensity. The parameter qP can also be interpreted as an estimate of the fraction of RCII in the open state, i.e. the primary stable electron acceptor in the oxidized state (Roháček, 2002). The number 6.022×10^{-3} converts $\mu\text{mol quanta to quanta and } 10^{-20} \text{ m}^2 \text{ to m}^2$.

Non-photochemical quenching (NPQ) at each light level was estimated as the normalized Stern–Volmer quenching coefficient, defined as $\text{NPQ}_{\text{NSV}} = (F'_m / F'_v) - 1 = F'_o / F'_v$ (McKew et al., 2013).

2.6 Carbon fixation

Rates of carbon fixation were measured as small volume P vs. E curves in a custom built photosynthetron as described in Schuback et al. (2015). Briefly, 300 mL water samples were spiked with 150 μCi $\text{NaH}^{14}\text{CO}_3$ (final concentration $0.5 \mu\text{Ci mL}^{-1}$, 52.5 mCi mL^{-1} specific activity) (Perkin–Elmer). Samples were spiked with tracer within 30 min of sampling, mixed gently but thoroughly, and then aliquoted into 20 mL glass scintillation vials and placed into the photosynthetron. Temperature was kept within 1°C of in situ temperature by circulating water from a water-bath through an aluminum cooling jacket. Each P vs. E curve consisted of 11 light levels spanning intensities from 3 to 600 $\mu\text{mol quanta m}^{-2} \text{s}^{-1}$. Incubations lasted for 3.5 h and were ended by gentle filtration onto pre-combusted 25 mm GF/F filters. All work was done under low light. For each curve, 3 time-zero samples were taken by filtering 20 mL immediately after adding the spike. The total ^{14}C activity added was determined from three 1 mL aliquots of the spiked sample added to 1 mL of 1 M NaOH. Filters were stored in scintillation vials at -20°C until processing within 1 month of the experiment. During laboratory processing, 500 μL of 3 M HCl was added to each filter and vials were left to degas for > 24 h to eliminate any inorganic ^{14}C remaining in the samples. Ten mL of scintillation cocktail (Scintisafe plus, Fisher) were added to each vial, and vials were then vortexed and left to stand in the dark for > 12 h before analysis on a liquid scintillation counter (Beckman). Disintegrations per minute (DPM) were derived from scintillation counts using a quench curve prepared from commercial ^{14}C standards (Perkin–Elmer). DPM were converted to units of carbon biomass following Knap et al. (1996).

BGD

12, 16803–16845, 2015

Diurnal variation in the coupling of photosynthetic electron transport

N. Schuback et al.

Title Page

Abstract

Introduction

Conclusions

References

Tables

Figures

◀

▶

◀

▶

Back

Close

Full Screen / Esc

Printer-friendly Version

Interactive Discussion



tion efficiency α , and the light saturation point $E_k = P_{\max}/\alpha$. When photoinhibition was observed at high irradiances, the data-points were excluded from the fitting procedure.

2.8 Derivation of conversion factor

The conversion factor linking ETR_{RCII} ($\text{mol e}^- \text{ mol RCII}^{-1} \text{ s}^{-1}$) and carbon fixation ($\text{mol C mol chl } a^{-1} \text{ s}^{-1}$), was derived as described in Schuback et al. (2015);

$$\frac{\text{ETR}_{\text{RCII}} \left(\text{mol e}^- \text{ mol RCII}^{-1} \text{ s}^{-1} \right)}{\text{C-fixation} \left(\text{mol C mol chl } a^{-1} \text{ s}^{-1} \right)} = \Phi_{\text{e:C}} \left(\frac{\text{mol e}^-}{\text{mol C}} \right) \times 1/n_{\text{PSII}} \left(\frac{\text{mol chl } a}{\text{mol RCII}} \right) \quad (6)$$

In this approach, the conversion factor between the two rates accounts for changes in chl a functionally associated with each RCII ($1/n_{\text{PSII}}$, $\text{mol chl } a \text{ mol RCII}^{-1}$), as well as variability in the number of charge separations in RCII needed per CO_2 assimilated ($\Phi_{\text{e:C}}$, $\text{mol e}^- \text{ mol C}^{-1}$). While an approach to estimate values of $1/n_{\text{PSII}}$ directly from FRRF measurements exists (Oxborough et al., 2012), it is unlikely to give accurate results under conditions of iron limitation (Behrenfeld and Milligan, 2013; Oxborough and Baker, 1997; Vassiliev et al., 1995), and has therefore not been applied in this study. Based on the measured light dependence of carbon fixation and ETR_{RCII} for each sample, we were able to derive the light dependency of the conversion factor $\Phi_{\text{e:C}}/n_{\text{PSII}}$ at each TP. Additionally, we used α and P_{\max} values from the ETR_{RCII} and ^{14}C P vs. E curves to derive the conversion factor under sub-saturating and saturating light conditions, respectively.

3 Results

3.1 Physical and chemical characteristics of the water-column during the experiment

During the sampling period, the upper water-column at OSP was stratified, with a well-defined mixed layer of 33 ± 2 m. As expected for iron-limited waters, excess macronutrients were present in the mixed layer and concentrations did not vary over the course of our sampling (2 casts, 3:30 and 12:30 LT; $N = 9.1 \pm 0.00 \mu\text{mol L}^{-1}$, $P = 0.98 \pm 0.01 \mu\text{mol L}^{-1}$, and $\text{Si} = 14.5 \pm 0.51 \mu\text{mol L}^{-1}$). Chlorophyll *a* concentrations were homogeneously distributed throughout the mixed layer ($0.26 \pm 0.03 \text{ mg m}^{-3}$; 8 depths sampled on 1 cast at 12:30 LT), while temperature was nearly invariant ($10.4 \pm 0.07^\circ\text{C}$) during our sampling period. Total daily incident PAR dose over the 24 h period (E_0^+) was $53\,236 \mu\text{mol quanta m}^{-2}$, with a noon maximum of $1162 \mu\text{mol quanta m}^{-2} \text{ s}^{-1}$. The water column light extinction coefficient, k_d , was 0.07 m^{-1} , which is a value typical for the open ocean (Kirk, 2010). The photic zone extended below the mixed layer depth at all TPs, apart from the nighttime TP (TPs 1, 7 and 8).

3.2 Phytoplankton community composition

CHEMTAX analysis of the pigment data suggested that the phytoplankton assemblage at the sampling location was highly diverse, consisting of approximately 3% diatoms, 2% dinoflagellates, 15% prymnesiophytes, 12% chlorophytes, 16% prasinophytes, 14% cryptophytes, 15% pelagophytes and 23% cyanobacteria.

3.3 Diurnal changes in rates of carbon fixation and ETR_{RCII}

Over the course of the diurnal cycle, we observed significant changes in the P vs. E curves for carbon fixation and ETR_{RCII} (Fig. 1). However, the two rates, and their light dependency, did not change in parallel (Fig. 1). As a consequence, we observed sig-

BGD

12, 16803–16845, 2015

Diurnal variation in the coupling of photosynthetic electron transport

N. Schuback et al.

Title Page

Abstract

Introduction

Conclusions

References

Tables

Figures

⏪

⏩

◀

▶

Back

Close

Full Screen / Esc

Printer-friendly Version

Interactive Discussion



an indicator of the activation of the photoprotective xanthophyll cycling process (Brunet et al., 2011).

The changes in pigment ratios shown in Fig. 5 indicate that the phytoplankton assemblage sampled from 5 m depth experienced supersaturating light conditions for a substantial part of the day. This is further confirmed by the diurnal changes in PSII-specific photophysiological parameters derived from FRRF measurements (Fig. 6). Estimates of the expression of non-photochemical quenching, NPQ_{NSV} , at in situ irradiance levels changed 7.6 fold over the diurnal cycle, with maximum values near the peak of solar irradiance (Fig. 6a). Spectrally corrected values of the functional absorption cross section of PSII, σ'_{PSII} , also derived for in situ irradiances, correlated inversely with irradiance (Fig. 6b). This decrease further confirms the induction of photo-protective mechanisms within the pigment antenna, preventing excess energy from reaching RCII. Values of F_v/F_m , measured in the dark-regulated state, varied from 0.12 to 0.32 and showed an inverse relationship to irradiance (Fig. 6c). Observed values of F_v/F_m are only about half of the values expected for nutrient deplete phytoplankton, confirming the iron-limited state of the phytoplankton assemblage sampled, while the diurnal changes likely indicate a down-regulation of PSII during high irradiance conditions. Photochemical quenching, qP, indicates the fraction of RCII in the “open state”, i.e. the primary stable electron acceptor Q_A in the oxidized state (Roháček, 2002). Values of qP, derived for a reference irradiance value of $500 \mu\text{mol quanta m}^{-2} \text{s}^{-1}$ at all TP, show significant change over the diurnal cycle, with mid-day values twice as high as those observed during the night (Fig. 6d).

4 Discussion

The experimental approach and results presented in this study contribute to a better understanding of environmentally driven shifts in cellular energy allocation that decouple photosynthesis from net growth on diurnal timescales. As the first study to investigate diurnal pattern of cellular energy allocation conducted in a HNLC region, our work also

BGD

12, 16803–16845, 2015

Diurnal variation in the coupling of photosynthetic electron transport

N. Schuback et al.

Title Page

Abstract

Introduction

Conclusions

References

Tables

Figures

◀

▶

◀

▶

Back

Close

Full Screen / Esc

Printer-friendly Version

Interactive Discussion



provides insight into how marine phytoplankton exploit their photophysiological plasticity to maximize growth while minimizing photodamage under iron-limited conditions.

In the following, we first discuss diurnal variation at the level of carbon fixation and put our observations in context with the rich information available from the literature.

We then consider the diurnal changes in ETR_{RCII} and the derived conversion factor $\Phi_{e:C}/\eta_{PSII}$, and discuss the relevance of our results to the development of FRRF-based phytoplankton primary productivity measurements. Building on the work of others (Behrenfeld et al., 2004, 2008; Halsey and Jones, 2015) we interpret our results in the context of cellular energy allocation.

4.1 Diurnal changes in carbon fixation

Diurnal variations in the capacity (P_{max}), efficiency (α) and realized rates of carbon fixation are characteristic of phytoplankton assemblages in the natural environment, as well as in laboratory cultures (Bruyant et al., 2005; Doblin et al., 2011; Doty and Oguri, 1957; Erga and Skjoldal, 1990; Harding et al., 1981, 1982, 1987; John et al., 2012; MacCaull and Platt, 1977; Prézelin, 1992; Stross et al., 1973; Zhao and Quigg, 2015). The general consensus is that carbon fixation is not passively regulated by the availability of light, but by complex metabolic feedbacks and endogenous circadian clocks. For example, it has been shown that expression of genes involved in carbon fixation peaks before dawn (Ashworth et al., 2013; Granum et al., 2009), “priming” cells to achieve maximum rates early in the day. High carbon fixation capacities before sunrise, as observed in our data (Fig. 2b), further confirm endogenous circadian control of this pathway.

In our data, P_{max} and α of carbon fixation peaked early in the morning and co-varied over the diurnal cycle (Fig. 2e and f). As a result, E_k (which is derived from the ratio of these parameters) remained relatively constant (Fig. 3). This “ E_k -independent” variability in the photosynthetic parameters P_{max} and α has long been considered somewhat enigmatic, but is now accepted to be driven by shifts in cellular energy allocation (Behrenfeld et al., 2004, 2008; Bruyant et al., 2005; Halsey and Jones, 2015).

Diurnal variation in the coupling of photosynthetic electron transport

N. Schuback et al.

Title Page

Abstract

Introduction

Conclusions

References

Tables

Figures



Back

Close

Full Screen / Esc

Printer-friendly Version

Interactive Discussion



In phytoplankton, the fraction of photosynthetically-derived reductant (NADPH) and energy equivalent (ATP) allocated to carbon fixation and net growth and the ratio of NADPH:ATP produced are finely tuned to match metabolic demand. Metabolic demand, in turn, is a function of evolved endogenous rhythms and external environmental forcing. As discussed below, the decline in P_{\max} (Fig. 2e), α (Fig. 2f), and realized rates of carbon fixation (Fig. 4c) after a peak in the early morning, are likely due to such shifts in energy allocation, as well as to the damaging effects of excess light, which accumulate throughout the light-period.

4.2 Diurnal changes in ETR_{RCII} and the conversion factor $\Phi_{e:C}/n_{PSII}$

In contrast to the diurnal cycles of P_{\max} and α of C-fixation, P_{\max} and α of ETR_{RCII} followed availability of light more closely, peaking at noon (Fig. 2c and d). Similarly, realized ETR_{RCII} , derived for in situ irradiances at each TP, correlated more closely to light availability than realized rates of carbon fixation (Fig. 4b). While it has been demonstrated that virtually all stages of photosynthesis exhibit circadian control (Suzuki and Johnson, 2001), our results suggests that ETR_{RCII} responds more directly to changes in light availability than the subsequent conversion of light energy into cellular organic carbon. The resulting decoupling of carbon fixation and photosynthetic electron transport is reflected in the diurnal variability in $\Phi_{e:C}/n_{PSII}$ (Figs. 2g and h, 4d).

In our dataset, in situ values for $\Phi_{e:C}/n_{PSII}$ ranged from 2700 to 9200 $\text{mole}^{-1} \text{molC mol chl } a \text{ mol RCII}^{-1}$. Assuming a constant value of 500 $\text{mol chl } a \text{ mol RCII}^{-1}$ (Kolber and Falkowski, 1993), the derived $\Phi_{e:C}$ ranges from 5–18 $\text{mole}^{-1} \text{molC}$, which is within the range of previously reported values (Lawrenz et al., 2013) and above the theoretical minimum of 4 $\text{mole}^{-1} \text{molC}$.

The large diurnal variability in ETR_{RCII} and carbon fixation and the highly variable $\Phi_{e:C}/n_{PSII}$, reflect the integrated growth environment experienced by the sampled phytoplankton assemblage. The lowest values of $\Phi_{e:C}/n_{PSII}$ were observed early in the morning (Fig. 4d), indicating that much of the energy harvested from sunlight and converted into chemical energy was used directly for carbon fixation. Thereafter, the

BGD

12, 16803–16845, 2015

Diurnal variation in the coupling of photosynthetic electron transport

N. Schuback et al.

Title Page

Abstract

Introduction

Conclusions

References

Tables

Figures

◀

▶

◀

▶

Back

Close

Full Screen / Esc

Printer-friendly Version

Interactive Discussion



conversion factor $\Phi_{e:C}/n_{PSII}$ increased rapidly, reaching a maximum in the afternoon (Fig. 4d).

On the cell physiological level, the increase in $\Phi_{e:C}/n_{PSII}$ can be explained by a number of interconnected mechanisms. Firstly, it is possible that diurnal oscillations in cell metabolism result in changes in organic carbon respiration and/or excretion. In our 3.5 h ^{14}C -uptake experiments, transient organic carbon pools destined for respiration or excretion could have been captured to different extents, affecting the derived conversion factor $\Phi_{e:C}/n_{PSII}$. Changes in cellular energy allocation, controlled in part by endogenous circadian rhythms, could also have affected the conversion factor $\Phi_{e:C}/n_{PSII}$, by re-routing NADPH and ATP generated by the photosynthetic light reaction to processes other than carbon fixation, thus increasing $\Phi_{e:C}/n_{PSII}$. Alternative sinks for ATP and NADPH formed during the light reaction are numerous and interconnected in complex ways, due to their differential demand for, and effect on, cellular ATP:NADPH ratios (Halsey and Jones, 2015). Processes decoupling ETR_{RCII} from carbon fixation include nutrient assimilation (Laws, 1991), carbon concentrating mechanisms (Giordano et al., 2005), photorespiration (Foyer et al., 2009), and malate formation (Halsey and Jones, 2015). Pseudo-cyclic electron transport through the Mehler-ascorbate peroxidase pathway also has the ability to increase the conversion factor $\Phi_{e:C}/n_{PSII}$ by allowing ETR_{RCII} to increase without affecting carbon fixation (Miyake and Asada, 2003; Niyogi, 2000). Moreover, processes acting before PSI can decouple ETR_{RCII} and carbon fixation by “siphoning” electrons out of the ETC to alleviate over-reduction under supersaturating light condition. Pseudo-cyclic electron transport through midstream terminal oxidases (Bailey et al., 2008; Mackey et al., 2008), cyclic electron transport around PSII (Feikema et al., 2006; Prasil et al., 1996), and charge recombination in RCII (Vass, 2011) could all be important under high mid-day irradiances, increasing ETR_{RCII} without affecting CO_2 -assimilation, and thus leading to a higher conversion factor $\Phi_{e:C}/n_{PSII}$.

Iron limitation, as experienced by the phytoplankton assemblage we sampled, directly affects the functioning of the ETC, which is rich in iron containing redox-chain

BGD

12, 16803–16845, 2015

Diurnal variation in the coupling of photosynthetic electron transport

N. Schuback et al.

Title Page

Abstract

Introduction

Conclusions

References

Tables

Figures

◀

▶

◀

▶

Back

Close

Full Screen / Esc

Printer-friendly Version

Interactive Discussion



components (Raven et al., 1999; Yruela, 2013). It is thus likely that the need for safe dissipation of excess excitation pressure after charge separation in RCII is enhanced under iron limitation (Behrenfeld and Milligan, 2013; Schuback et al., 2015), leading to a greater decoupling of ETR_{RCII} and carbon fixation (Schuback et al., 2015). Pseudo-cyclic electron flow could alleviate over-reduction of the ETC under iron limiting conditions, while also contributing to ATP production (Behrenfeld and Milligan, 2013). The resulting increase in the cellular ATP : NADPH ratio would match the shift in energy demand from growth (higher NADPH requirement) to maintenance (higher ATP requirement), which takes place under nutrient limited growth conditions.

In conclusion, we suggest that the observed changes in the conversion factor $\Phi_{e:C}/n_{PSII}$ over the diurnal cycle reflect the interactions of external phasing of photosynthetic metabolism by the availability of light as well as internal metabolic rhythms in cell metabolism, optimizing energy allocation and growth under iron-limited conditions.

4.3 Diurnal changes in photophysiology at the level of PSII

In our data, several lines of evidence demonstrate that the phytoplankton assemblage we sampled from 5 m depth experienced supersaturating irradiance during part of the day. A suite of mechanisms was activated to dissipate the excess excitation energy in the pigment antenna, before it could reach RCII. This was indicated by changes in pigment ratios and FRRF-derived photophysiological parameters (Figs. 5 and 6). The light harvesting antennae of phytoplankton are comprised of both photosynthetic and photoprotective pigments, the relative abundance of which can change in response to irradiance. The ratio $[PPC]/[TPig]$, provides information on the degree of high light acclimation of a mixed phytoplankton assemblage (Brunet et al., 2011). In our data, $[PPC]/[TPig]$ increased during the day (Fig. 5a), indicating that the phytoplankton assemblage experienced and responded to supersaturating irradiance levels. Furthermore, significant changes in the DES ratio (Fig. 5b) illustrate rapid activation of photo-

BGD

12, 16803–16845, 2015

Diurnal variation in the coupling of photosynthetic electron transport

N. Schuback et al.

Title Page

Abstract

Introduction

Conclusions

References

Tables

Figures

◀

▶

◀

▶

Back

Close

Full Screen / Esc

Printer-friendly Version

Interactive Discussion



protective energy dissipation in the pigment antenna in response to diurnal changes in irradiance (Brunet et al., 2011).

Processes that dissipate excess excitation pressure in the pigment antenna also quench ChlF yields measured by FRRF. Therefore, non-photochemical quenching (NPQ), as estimated from FRRF measurements, has been widely used as an estimate for photoprotective energy dissipation (Demmig-Adams et al., 2014; Derks et al., 2015). NPQ encompasses a wide variety of mechanisms, all acting to dissipate absorbed light energy as heat before it reaches RCII (e.g. Derks et al., 2015). Following the approach of McKew et al. (2013) we estimated NPQ from FRRF measurements as so-called normalized Stern–Volmer quenching (NPQ_{NSV}). The 7.6 fold change in NPQ_{NSV} , estimated for in situ light availability at 5 m depth (Fig. 6a), confirms that the phytoplankton assemblage sampled experienced, and rapidly reacted to, super-saturating light conditions. The inverse light dependence of σ'_{PSII} , (functional absorption cross-section of PSII) derived for in situ irradiances at each TP (Fig. 6b), provides a further illustration of rapid changes taking place in the pigment antenna to prevent excess excitation energy from reaching RCII.

Throughout the diurnal cycle, values of F_v/F_m , derived for the dark-regulated state, were low, confirming the iron-limited state of the phytoplankton assemblage (Fig. 6c) (Petrou et al., 2011; Behrenfeld and Milligan, 2013). The decrease in F_v/F_m at noon, however, is not due to changes in the nutritional state of the phytoplankton, but to persistent photo-protective changes and photoinhibition in PSII (Öquist et al., 1992). In order to derive ChlF yields and parameters in the dark-regulated state, samples are typically left in the dark or low light before measurements. This “dark-acclimation” is meant to allow for oxidation of the ETC and relaxation of all NPQ processes, enabling the measurement of maximum ChlF yields. In practice, however, a fully dark-regulated state cannot be achieved in mixed phytoplankton assemblages in the field, where optimal dark-acclimation times can be on the order of hours long (From et al., 2014), and would depend on recent light history and taxonomic composition. Despite this ambiguity in the derivation of F_v/F_m , the observed inverse relationship to diurnal light

Diurnal variation in the coupling of photosynthetic electron transport

N. Schuback et al.

Title Page

Abstract

Introduction

Conclusions

References

Tables

Figures



Back

Close

Full Screen / Esc

Printer-friendly Version

Interactive Discussion



availability strongly indicates the presence of slow-relaxing NPQ components (including damage of PSII protein), providing further evidence for high light stress experienced by the phytoplankton assemblage (Fig. 6c).

In addition to the protective mechanisms discussed above, which act in the pigment antenna to prevent charge separation in RCII, photo-protective mechanisms also act after charge separation in RCII (Sect. 4.2). These mechanisms alleviate over-reduction by allowing rapid re-oxidation of the primary stable electron acceptor Q_A . Our data show evidence of the up-regulation of such alternative electron sinks during mid-day. Figure 6d shows values of the estimated fraction of Q_A in the oxidized state (qP). Importantly, these values of qP were derived for a reference irradiance of $500 \mu\text{mol quanta m}^{-2} \text{s}^{-1}$. The mid-day increase in the oxidized fraction of Q_A at a constant saturating irradiance of $500 \mu\text{mol quanta m}^{-2} \text{s}^{-1}$ strongly suggests the up-regulation of alternative electron sinks, which most likely serve a photoprotective function (Mackey et al., 2008). Importantly, up-regulation of these processes directly affect the conversion factor $\Phi_{e:C}/n_{\text{PSII}}$ (Sect. 4.2).

4.4 Linking $\Phi_{e:C}/n_{\text{PSII}}$ and NPQ_{NSV}

Considering that processes preventing energy transfer to RCII and processes acting to prevent over-reduction of the ETC after charge separation are all driven by excess excitation energy, it is reasonable to expect that their magnitude correlates. Following the approach and interpretation suggested by Schuback et al. (2015), we examined the correlation between the derived conversion factor $\Phi_{e:C}/n_{\text{PSII}}$ and estimates of NPQ_{NSV} . As shown in Fig. 7, we found a strong correlation between these two variables ($R^2 = 0.81$, p value < 0.0001 , $n = 64$). Data shown in Fig. 7 are estimates of NPQ_{NSV} for each light level of the FRRF light curves at each TP. For the same light levels, we derived values of $\Phi_{e:C}/n_{\text{PSII}}$ by extrapolation along the carbon fixation and ETR_{RCII} based P vs. E curves.

BGD

12, 16803–16845, 2015

Diurnal variation in the coupling of photosynthetic electron transport

N. Schuback et al.

Title Page

Abstract

Introduction

Conclusions

References

Tables

Figures

◀

▶

◀

▶

Back

Close

Full Screen / Esc

Printer-friendly Version

Interactive Discussion



Diurnal variation in the coupling of photosynthetic electron transport

N. Schuback et al.

Title Page

Abstract

Introduction

Conclusions

References

Tables

Figures

◀

▶

◀

▶

Back

Close

Full Screen / Esc

Printer-friendly Version

Interactive Discussion

As described in detail in Schuback et al. (2015), the correlation between $\Phi_{e:C}/n_{PSII}$ and NPQ_{NSV} can be mechanistically explained by the effects of excess excitation pressure and consequent expression of protective mechanisms both upstream and downstream of charge separation in RCII. The dissipation of excess excitation energy as thermal energy before reaching RCII, estimated as NPQ_{NSV} , prevents excess electron transport and over-reduction of the ETC. After the initial charge separation in RCII, excess electron transport and over-reduction of the ETC can be alleviated by a number of alternative electron pathways; the up-regulation of which will increase $\Phi_{e:C}/n_{PSII}$ (e.g. Bailey et al., 2008; Cardol et al., 2011; Laureau et al., 2013; Mackey et al., 2008; McDonald et al., 2011; Niyogi, 2000; Streb et al., 2005; Vass, 2011; Zehr and Kudela, 2009). Thus, both NPQ_{NSV} and $\Phi_{e:C}/n_{PSII}$ respond strongly to excess excitation pressure, providing a mechanistic interpretation for their tight correlation. In fact, a positive feedback loop exists between energy dissipation in the antenna and photosynthetic control in the ETC, because alternative electron pathways enhance the trans-membrane Δ -pH, which triggers several components of NPQ (Nawrocki et al., 2015).

As expected, both NPQ_{NSV} and $\Phi_{e:C}/n_{PSII}$ were highest at midday and during the early afternoon, coinciding with highest irradiance levels (Fig. 7, black symbols). Similarly, values measured during the night-time TPs showed low values for both, NPQ_{NSV} and $\Phi_{e:C}/n_{PSII}$ (Fig. 7, white symbols). Interestingly, during the early morning (6:00 LT, grey circles in Fig. 7), NPQ_{NSV} increased more rapidly than $\Phi_{e:C}/n_{PSII}$, while $\Phi_{e:C}/n_{PSII}$ increased more rapidly than NPQ_{NSV} during the late afternoon (21:00 LT, grey diamonds in Fig. 7). Mechanistically, these observations may be explained by the differential induction and relaxation time-scales of the different photo-protective mechanisms involved. NPQ_{NSV} , which represents rapid changes in the pigment antenna, may be activated earlier in the diurnal cycle, while the dissipation of excess excitation energy by processes acting after charge separation in RCII appear to lag in both induction and relaxation. The importance of multiple interacting photo-protective mechanisms, acting

on different timescales, has recently been discussed by e.g. Derks et al. (2015) and Giovagnetti et al. (2014).

While a correlation between NPQ_{NSV} and $\Phi_{\text{e:C}}/n_{\text{PSII}}$ can be mechanistically explained and could have important implications for the derivation of primary productivity rates in carbon units from FRRF measurements, it can be confounded by ambiguity and inherent biases in the derivation of all involved parameters. For example, while the correlations between NPQ_{NSV} and $\Phi_{\text{e:C}}/n_{\text{PSII}}$ in the present, as well as our previously published dataset (Schuback et al., 2015), are strong, the slopes of the relationships differ. The observed discrepancy could be explained in several ways. Firstly, data in our previous study was not corrected for spectral differences between the FRRF instrument, the ^{14}C -uptake experiments and in situ light. As a consequence, absolute values of the derived conversion factor were likely over-estimated. Furthermore, data presented in Schuback et al. (2015) included phytoplankton assemblages sampled over a range of iron-limited and iron-replete conditions, likely resulting in a range of growth rates that would influence the relative balance between net and gross carbon fixation captured in 3 h ^{14}C -uptake experiments (Halsey et al., 2011; Milligan et al., 2015; Pei and Laws, 2013), and affect the derived conversion factor $\Phi_{\text{e:C}}/n_{\text{PSII}}$.

More generally, significant uncertainty remains in the estimation of ETR_{RCII} from ChlF yields, particularly if the theoretical biophysical models are applied to mixed phytoplankton assemblages containing species with contrasting photosynthetic architectures and photo-physiological characteristics. Inherent biases, and potential systematic errors in the derivation of ETR_{RCII} will inevitably affect the derived conversion factor $\Phi_{\text{e:C}}/n_{\text{PSII}}$. Similarly, it remains unclear if the quenching of ChlF yields, used to derive NPQ, correlate linearly with increases in thermal energy dissipation in the pigment antenna (Derks et al., 2015). Larger datasets, spanning multiple oceanic regions and phytoplankton assemblages of contrasting taxonomic composition and physiological state are needed to further investigate the correlation between NPQ_{NSV} and $\Phi_{\text{e:C}}/n_{\text{PSII}}$.

BGD

12, 16803–16845, 2015

Diurnal variation in the coupling of photosynthetic electron transport

N. Schuback et al.

Title Page

Abstract

Introduction

Conclusions

References

Tables

Figures

◀

▶

◀

▶

Back

Close

Full Screen / Esc

Printer-friendly Version

Interactive Discussion



5 Conclusions

The lure of FRRF instruments lies in their potential for autonomous, instantaneous data acquisition at high temporal and spatial resolution. However, uncertainty in the conversion factor needed to convert rates of ETR_{RCII} into ecologically relevant rates of carbon fixation remains a significant challenge. Through a suite of photo-physiological data and ancillary measurements, our results provide some insight into the potential mechanistic causes leading to an uncoupling of ETR_{RCII} and carbon fixation over diurnal cycles in iron-limited phytoplankton assemblages. We suggest that recent efforts to estimate the conversion factor from predominant environmental conditions (Lawrenz et al., 2013), could potentially be improved using the observed strong correlation between the derived conversion factor and NPQ_{NSV} . Beyond providing improved methods to estimate phytoplankton carbon fixation rates, information on magnitude and variability of the conversion factor linking ETR_{RCII} and carbon fixation allows a better mechanistic understanding of how phytoplankton harvest and allocate light energy in response to environmental conditions. Our mechanistic understanding of these processes is crucial for the modeling and prediction of patterns in marine primary productivity in the face of climate-dependent changes in oceanic ecosystems.

More generally, it is important to consider that the dynamics of marine productivity over long time-scales are ultimately controlled by interactions among biological and physical processes that have strong diurnal components. Several recent studies suggest a previously under-appreciated importance of closely coupled diurnal oscillations as the underlying mechanisms of ecosystem stability in open ocean food webs (Ottosen et al., 2014; Ribalet et al., 2015). Our results show strong diurnal variability in photophysiology and cell metabolism of mixed phytoplankton assemblages. These physiological processes likely influence the phasing and periodicity of higher trophic level processes, and may ultimately contribute to conveying stability to the system.

Acknowledgements. The authors thank Marie Robert and the scientific and coast guard crews on board CCGS *John P. Tully* during Line-P 2014-18. We would further like to thank Z. Kolber for

BGD

12, 16803–16845, 2015

Diurnal variation in the coupling of photosynthetic electron transport

N. Schuback et al.

Title Page

Abstract

Introduction

Conclusions

References

Tables

Figures



Back

Close

Full Screen / Esc

Printer-friendly Version

Interactive Discussion



assistance with the FRRF instrument and C. Hoppe and D. Semeniuk for their critical reading of the manuscript.

References

- 5 Arrigo, K. R., Mills, M. M., Kropuenske, L. R., Dijken, G. L. van, Alderkamp, A.-C., and Robinson, D. H.: Photophysiology in two major southern ocean phytoplankton taxa: photosynthesis and growth of *Phaeocystis antarctica* and *Fragilariopsis cylindrus* under different irradiance levels, *Integr. Comp. Biol.*, 50, 950–966, doi:10.1093/icb/icq021, 2010.
- Ashworth, J., Coesel, S., Lee, A., Armbrust, E. V., Orellana, M. V., and Baliga, N. S.: Genome-wide diel growth state transitions in the diatom *Thalassiosira pseudonana*, *P. Natl. Acad. Sci. USA*, 110, 7518–7523, doi:10.1073/pnas.1300962110, 2013.
- 10 Babin, M., Morel, A., Claustre, H., Bricaud, A., Kolber, Z., and Falkowski, P. G.: Nitrogen- and irradiance-dependent variations of the maximum quantum yield of carbon fixation in eutrophic, mesotrophic and oligotrophic marine systems, *Deep-Sea Res.*, 43, 1241–1272, doi:10.1016/0967-0637(96)00058-1, 1996.
- 15 Bailey, S., Melis, A., Mackey, K. R. M., Cardol, P., Finazzi, G., van Dijken, G., Berg, G. M., Arrigo, K., Shrager, J., and Grossman, A.: Alternative photosynthetic electron flow to oxygen in marine *Synechococcus*, *Biochim. Biophys. Acta*, 1777, 269–276, doi:10.1016/j.bbabi.2008.01.002, 2008.
- Barwell-Clarke, F. W.: Institute of Ocean Sci.s Nutrient Methods and Analysis, *Can. Tech. Rep. Hydrogr. Ocean Sci.*, 182, 43 pp., 1996.
- 20 Behrenfeld, M. J. and Milligan, A. J.: Photophysiological expressions of iron stress in phytoplankton, *Annu. Rev. Mar. Sci.*, 5, 217–246, doi:10.1146/annurev-marine-121211-172356, 2013.
- Behrenfeld, M. J., Prasil, O., Babin, M., and Bruyant, F.: In search of a physiological basis for covariations in light-limited and light-saturated photosynthesis, *J. Phycol.*, 40, 4–25, 2004.
- 25 Behrenfeld, M. J., Halsey, K. H., and Milligan, A. J.: Evolved physiological responses of phytoplankton to their integrated growth environment, *Philos. Trans. R. Soc. B*, 363, 2687–2703, 2008.

Diurnal variation in the coupling of photosynthetic electron transport

N. Schuback et al.

Title Page

Abstract

Introduction

Conclusions

References

Tables

Figures



Back

Close

Full Screen / Esc

Printer-friendly Version

Interactive Discussion



Diurnal variation in the coupling of photosynthetic electron transport

N. Schuback et al.

Title Page

Abstract

Introduction

Conclusions

References

Tables

Figures



Back

Close

Full Screen / Esc

Printer-friendly Version

Interactive Discussion



- Brunet, C., Johnsen, G., Lavaud, J., and Roy, S.: Pigments and photoacclimation processes, *Phytoplankton Pigments Charact. Chemotaxon. Appl. Oceanogr.*, available at: <https://hal.archives-ouvertes.fr/hal-01101814/> (last access: 29 August 2015), 2011.
- 5 Bruyant, F., Babin, M., Genty, B., Prasil, O., Behrenfeld, M. J., Claustre, H., Bricaud, A., Garczarek, L., Holtzendorff, J., and Koblizek, M.: Diel variations in the photosynthetic parameters of *Prochlorococcus* strain PCC 9511: combined effects of light and cell cycle, *Limnol. Oceanogr.*, 50, 850–863, 2005.
- Cardol, P., Forti, G., and Finazzi, G.: Regulation of electron transport in microalgae, *Biochim. Biophys. Acta*, 1807, 912–918, 2011.
- 10 Cheah, W., McMinn, A., Griffiths, F. B., Westwood, K. J., Wright, S. W., Molina, E., Webb, J. P., and van den Eenden, R.: Assessing Sub-Antarctic Zone primary productivity from fast repetition rate fluorometry, *Deep-Sea Res. Pt. II*, 58, 2179–2188, doi:10.1016/j.dsr2.2011.05.023, 2011.
- Corno, G., Letelier, R. M., Abbott, M. R., and Karl, D. M.: Assessing primary production variability in the North Pacific Subtropical Gyre: a comparison of fast repetition rate fluorometry and ^{14}C measurements, *J. Phycol.*, 42, 51–60, 2006.
- 15 Demmig-Adams, B., Garab, G., Adams III, W., and Govindjee (Eds.): *Non-Photochemical Quenching and Energy Dissipation in Plants, Algae and Cyanobacteria*, Springer Netherlands, Dordrecht, available at: <http://link.springer.com/10.1007/978-94-017-9032-1> (last access: 9 June 2015), 2014.
- 20 Derks, A., Schaven, K., and Bruce, D.: Diverse mechanisms for photoprotection in photosynthesis. Dynamic regulation of photosystem II excitation in response to rapid environmental change, *Biochim. Biophys. Acta*, 1847, 468–485, doi:10.1016/j.bbabi.2015.02.008, 2015.
- Doblin, M. A., Petrou, K. L., Shelly, K., Westwood, K., van den Eenden, R., Wright, S., Griffiths, B., and Ralph, P. J.: Diel variation of chlorophyll *a* fluorescence, phytoplankton pigments and productivity in the Sub-Antarctic and Polar Front Zones south of Tasmania, Australia, *Deep-Sea Res. Pt. II*, 58, 2189–2199, doi:10.1016/j.dsr2.2011.05.021, 2011.
- 25 Doty, M. S. and Oguri, M.: Evidence for a photo synthetic daily periodicity, *Limnol. Oceanogr.*, 2, 37–40, doi:10.4319/lo.1957.2.1.0037, 1957.
- 30 Erga, S. R. and Skjoldal, H. R.: Diel variations in photosynthetic activity of summer phytoplankton in Linda aspollene, western Norway, available at: <http://brage.bibsys.no/xmlui/handle/11250/108310> (last access: 8 September 2015), 1990.

Diurnal variation in the coupling of photosynthetic electron transport

N. Schuback et al.

Title Page

Abstract

Introduction

Conclusions

References

Tables

Figures



Back

Close

Full Screen / Esc

Printer-friendly Version

Interactive Discussion

- Feikema, O. W., Marosvölgyi, M. A., Lavaud, J., and van Gorkom, H. J.: Cyclic electron transfer in photosystem II in the marine diatom *Phaeodactylum tricornutum*, *Biochim. Biophys. Acta*, 1757, 829–834, doi:10.1016/j.bbabi.2006.06.003, 2006.
- Field, C. B., Behrenfeld, M. J., Randerson, J. T., and Falkowski, P.: Primary production of the biosphere: integrating terrestrial and oceanic components, *Science*, 281, 237–240, 1998.
- Foyer, C. H., Bloom, A. J., Queval, G., and Noctor, G.: Photorespiratory metabolism: genes, mutants, energetics, and redox signaling, *Annu. Rev. Plant Biol.*, 60, 455–484, doi:10.1146/annurev.arplant.043008.091948, 2009.
- From, N., Richardson, K., Mousing, E. A., and Jensen, P. E.: Removing the light history signal from normalized variable fluorescence (F_v/F_m) measurements on marine phytoplankton, *Limnol. Oceanogr.-Meth.*, 12, 776–783, doi:10.4319/lom.2014.12.776, 2014.
- Fujiki, T., Suzue, T., Kimoto, H., and Saino, T.: Photosynthetic electron transport in *Dunaliella tertiolecta* (Chlorophyceae) measured by fast repetition rate fluorometry: relation to carbon assimilation, *J. Plankton Res.*, 29, 199–208, 2007.
- Giordano, M., Beardall, J., and Raven, J. A.: CO₂ concentrating mechanisms in algae: mechanisms, environmental modulation, and evolution, *Annu. Rev. Plant Biol.*, 56, 99–131, doi:10.1146/annurev.arplant.56.032604.144052, 2005.
- Giovagnetti, V., Flori, S., Tramontano, F., Lavaud, J., and Brunet, C.: The velocity of light intensity increase modulates the photoprotective response in coastal diatoms, *PLoS ONE*, 9, e103782, doi:10.1371/journal.pone.0103782, 2014.
- Goto, N., Miyazaki, H., Nakamura, N., Terai, H., Ishida, N., and Mitamura, O.: Relationships between electron transport rates determined by pulse amplitude modulated (PAM) chlorophyll fluorescence and photosynthetic rates by traditional and common methods in natural freshwater phytoplankton, *Fundam. Appl. Limnol. Arch. Fr Hydrobiol.*, 172, 121–134, doi:10.1127/1863-9135/2008/0172-0121, 2008.
- Granum, E., Roberts, K., Raven, J. A., and Leegood, R. C.: Primary carbon and nitrogen metabolic gene expression in the diatom *Thalassiosira Pseudonana* (bacillariophyceae): diel periodicity and effects of inorganic carbon and nitrogen, *J. Phycol.*, 45, 1083–1092, doi:10.1111/j.1529-8817.2009.00728.x, 2009.
- Halsey, K. H. and Jones, B. M.: Phytoplankton strategies for photosynthetic energy allocation, *Annu. Rev. Mar. Sci.*, 7, 265–297, doi:10.1146/annurev-marine-010814-015813, 2015.

Diurnal variation in the coupling of photosynthetic electron transport

N. Schuback et al.

Title Page

Abstract

Introduction

Conclusions

References

Tables

Figures



Back

Close

Full Screen / Esc

Printer-friendly Version

Interactive Discussion



- Halsey, K. H., Milligan, A. J., and Behrenfeld, M. J.: Linking time-dependent carbon-fixation efficiencies in *Dunaliella Tertiolecta* (chlorophyceae) to underlying metabolic pathways, *J. Phycol.*, 47, 66–76, doi:10.1111/j.1529-8817.2010.00945.x, 2011.
- Harding, L. W., Meeson, B. W., Prézelin, B. B., and Sweeney, B. M.: Diel periodicity of photosynthesis in marine phytoplankton, *Mar. Biol.*, 61, 95–105, doi:10.1007/BF00386649, 1981.
- Harding, L. W., Prézelin, B. B., Sweeney, B. M., and Cox, J. L.: Primary production as influenced by diel periodicity of phytoplankton photosynthesis, *Mar. Biol.*, 67, 179–186, 1982.
- Harding, L. W., Fisher, T. R., and Tyler, M. A.: Adaptive responses of photosynthesis in phytoplankton: specificity to time-scale of change in light, *Biol. Oceanogr.*, 4, 403–437, doi:10.1080/01965581.1987.10749499, 1987.
- John, D. E., López-Díaz, J. M., Cabrera, A., Santiago, N. A., Corredor, J. E., Bronk, D. A., and Paul, J. H.: A day in the life in the dynamic marine environment: how nutrients shape diel patterns of phytoplankton photosynthesis and carbon fixation gene expression in the Mississippi and Orinoco River plumes, *Hydrobiologia*, 679, 155–173, 2012.
- Kaiblinger, C. and Dokulil, M. T.: Application of fast repetition rate fluorometry to phytoplankton photosynthetic parameters in freshwaters, *Photosynth. Res.*, 88, 19–30, 2006.
- Kirk, J. T. O.: *Light and Photosynthesis in Aquatic Ecosystems*, Cambridge University Press, Cambridge, 2011.
- Kishino, M., Takahashi, M., Okami, N., and Ichimura, S.: Estimation of the spectral absorption coefficients of phytoplankton in the sea, *Bull. Mar. Sci.*, 37, 634–642, 1985.
- Knap, A. H., Michaels, A., Close, A. R., Ducklow, H., and Dickson, A. G.: Protocols for the joint global ocean flux study (JGOFS) core measurements, JGOFS Repr. IOC Man. Guid. No 29 UNESCO 1994, 19, available at: <http://epic.awi.de/17559/1/Kna1996a.pdf> (last access: 15 October 2014), 1996.
- Kolber, Z. and Falkowski, P. G.: Use of active fluorescence to estimate phytoplankton photosynthesis in situ, *Limnol. Oceanogr.*, 38, 1646–1665, doi:10.4319/lo.1993.38.8.1646, 1993.
- Kolber, Z. S., Prášil, O., and Falkowski, P. G.: Measurements of variable chlorophyll fluorescence using fast repetition rate techniques: defining methodology and experimental protocols, *Biochim. Biophys. Acta*, 1367, 88–106, doi:10.1016/S0005-2728(98)00135-2, 1998.
- Laureau, C., DE Paepe, R., Latouche, G., Moreno-Chacón, M., Finazzi, G., Kuntz, M., Cornic, G., and Streb, P.: Plastid terminal oxidase (PTOX) has the potential to act as a safety valve for excess excitation energy in the alpine plant species *Ranunculus glacialis* L., *Plant Cell Environ.*, 36, 1296–1310, doi:10.1111/pce.12059, 2013.

Diurnal variation in the coupling of photosynthetic electron transport

N. Schuback et al.

Title Page

Abstract

Introduction

Conclusions

References

Tables

Figures



Back

Close

Full Screen / Esc

Printer-friendly Version

Interactive Discussion



- Lawrenz, E., Silsbe, G., Capuzzo, E., Ylöstalo, P., Forster, R. M., Simis, S. G. H., Prášil, O., Kromkamp, J. C., Hickman, A. E., Moore, C. M., Forget, M.-H., Geider, R. J., and Suggett, D. J.: Predicting the electron requirement for carbon fixation in seas and oceans, *PLoS ONE*, 8, e58137, doi:10.1371/journal.pone.0058137, 2013.
- 5 Laws, E. A.: Photosynthetic quotients, new production and net community production in the open ocean, *Deep-Sea Res.*, 38, 143–167, 1991.
- Lee, Y. W., Park, M. O., Kim, Y. S., Kim, S. S., and Kang, C. K.: Application of photosynthetic pigment analysis using a HPLC and CHEMTAX program to studies of phytoplankton community composition, *J. Korean Soc. Ocean.*, 16, 117–124, 2011.
- 10 MacCaull, W. A. and Platt, T.: Diel variations in the photosynthetic parameters of coastal marine phytoplankton, *Limnol. Oceanogr.*, 22, 723–731, doi:10.4319/lo.1977.22.4.0723, 1977.
- Mackey, K. R. M., Paytan, A., Grossman, A. R., and Bailey, S.: A photosynthetic strategy for coping in a high-light, low-nutrient environment, *Limnol. Oceanogr.*, 53, 900–913, doi:10.4319/lo.2008.53.3.0900, 2008.
- 15 McDonald, A. E., Ivanov, A. G., Bode, R., Maxwell, D. P., Rodermel, S. R., and Hüner, N. P. A.: Flexibility in photosynthetic electron transport: the physiological role of plastoquinol terminal oxidase (PTOX), *Biochim. Biophys. Acta*, 1807, 954–967, doi:10.1016/j.bbabi.2010.10.024, 2011.
- McKew, B. A., Davey, P., Finch, S. J., Hopkins, J., Lefebvre, S. C., Metodiev, M. V., Oxborough, K., Raines, C. A., Lawson, T., and Geider, R. J.: The trade-off between the light-harvesting and photoprotective functions of fucoxanthin-chlorophyll proteins dominates light acclimation in *Emiliania huxleyi* (clone CCMP 1516), *New Phytol.*, 200, 74–85, doi:10.1111/nph.12373, 2013.
- 20 Milligan, A. J., Halsey, K. H., and Behrenfeld, M. J.: Advancing interpretations of ¹⁴C-uptake measurements in the context of phytoplankton physiology and ecology, *J. Plankton Res.*, 37, 692–698, doi:10.1093/plankt/fbv051, 2015.
- 25 Mitchell, B. G., Kahru, M., Wieland, J., and Stramska, M.: Determination of spectral absorption coefficients of particles, dissolved material and phytoplankton for discrete water samples, *Ocean Opt. Protoc. Satell. Ocean Color Sens. Valid. Revis.*, 3, 231–257, 2002.
- 30 Miyake, C. and Asada, K.: The water-water cycle in algae, in: *Photosynthesis in Algae*, edited by: Larkum, A. W. D., Douglas, S. E., and Raven, J. A., 183–204, Springer, the Netherlands, available at: http://link.springer.com/chapter/10.1007/978-94-007-1038-2_9 (last access: 10 March 2015), 2003.

Diurnal variation in the coupling of photosynthetic electron transport

N. Schuback et al.

Title Page

Abstract

Introduction

Conclusions

References

Tables

Figures

◀

▶

◀

▶

Back

Close

Full Screen / Esc

Printer-friendly Version

Interactive Discussion



- Morel, A., Gentili, B., Claustre, H., Babin, M., Bricaud, A., Ras, J., and Tièche, F.: Optical properties of the “clearest” natural waters, *Limnol. Oceanogr.*, 52, 217–229, doi:10.4319/lo.2007.52.1.0217, 2007.
- Myers, J.: On the algae: thoughts about physiology and measurements of efficiency, in: *Primary Productivity in the Sea*, edited by: Falkowski, P. G., 1–16, Springer, New York, US, available at: http://link.springer.com/chapter/10.1007/978-1-4684-3890-1_1 (last access: 28 August 2015), 1980.
- Napoléon, C. and Claquin, P.: Multi-parametric relationships between PAM measurements and carbon incorporation, an in situ approach, *PloS One*, 7, e40284, doi:10.1371/journal.pone.0040284, 2012.
- Napoléon, C., Raimbault, V., and Claquin, P.: Influence of nutrient stress on the relationships between PAM measurements and carbon incorporation in four phytoplankton species, *PloS One*, 8, e66423, doi:10.1371/journal.pone.0066423, 2013.
- Nawrocki, W. J., Tourasse, N. J., Taly, A., Rappaport, F., and Wollman, F.-A.: The plastid terminal oxidase: its elusive function points to multiple contributions to plastid physiology, *Annu. Rev. Plant Biol.*, 66, 49–74, doi:10.1146/annurev-arplant-043014-114744, 2015.
- Niyogi, K. K.: Safety valves for photosynthesis, *Curr. Opin. Plant Biol.*, 3, 455–460, doi:10.1016/S1369-5266(00)00113-8, 2000.
- Öquist, G., Chow, W. S., and Anderson, J. M.: Photoinhibition of photosynthesis represents a mechanism for the long-term regulation of photosystem II, *Planta*, 186, 450–460, doi:10.1007/BF00195327, 1992.
- Ottesen, E. A., Young, C. R., Gifford, S. M., Eppley, J. M., Marin, R., Schuster, S. C., Scholin, C. A., and DeLong, E. F.: Multispecies diel transcriptional oscillations in open ocean heterotrophic bacterial assemblages, *Science*, 345, 207–212, doi:10.1126/science.1252476, 2014.
- Oxborough, K. and Baker, N. R.: Resolving chlorophyll *a* fluorescence images of photosynthetic efficiency into photochemical and non-photochemical components – calculation of qP and F'_V/F'_m ; without measuring F'_o , *Photosynth. Res.*, 54, 135–142, doi:10.1023/A:1005936823310, 1997.
- Oxborough, K., Moore, C. M., Suggett, D. J., Lawson, T., Chan, H. G., and Geider, R. J.: Direct estimation of functional PSII reaction center concentration and PSII electron flux on a volume basis: a new approach to the analysis of Fast Repetition Rate fluorometry (FRRf) data, *Limnol Ocean. Methods*, 10, 142–154, 2012.

tron transport and CO₂-assimilation in marine phytoplankton, PLoS ONE, 10, e0133235, doi:10.1371/journal.pone.0133235, 2015.

Silsbe, G.: Phytotools: Phytoplankton Production Tools, , An R package available on CRAN: <https://cran.r-project.org/web/packages/phytotools/index.html>, 2015.

5 Streb, P., Josse, E.-M., Gallouët, E., Baptist, F., Kuntz, M., and Cornic, G.: Evidence for alternative electron sinks to photosynthetic carbon assimilation in the high mountain plant species *Ranunculus glacialis*, Plant Cell Environ., 28, 1123–1135, doi:10.1111/j.1365-3040.2005.01350.x, 2005.

10 Stross, R. G., Chisholm, S. W., and Downing, T. A.: Causes of daily rhythms in photosynthetic rates of phytoplankton, Biol. Bull., 145, 200–209, doi:10.2307/1540359, 1973.

Suggett, D., Kraay, G., Holligan, P., Davey, M., Aiken, J., and Geider, R.: Assessment of photosynthesis in a spring cyanobacterial bloom by use of a fast repetition rate fluorometer, Limnol. Oceanogr., 46, 802–810, 2001.

15 Suggett, D. J., Moore, C. M., and Geider, R. J.: Estimating aquatic productivity from active fluorescence measurements, in: Chlorophyll *a* Fluorescence in Aquatic Sciences: Methods and Applications, edited by: Suggett D. J., Prasil O., and Borowitzka M. A., 103–127, Springer, the Netherlands, 2010.

Suzuki, L. and Johnson, C. H.: Algae know the time of day: circadian and photoperiodic programs, J. Phycol., 37, 933–942, doi:10.1046/j.1529-8817.2001.01094.x, 2001.

20 Taylor, R. L., Semeniuk, D. M., Payne, C. D., Zhou, J., Tremblay, J.-É., Cullen, J. T., and Maldonado, M. T.: Colimitation by light, nitrate, and iron in the Beaufort Sea in late summer, J. Geophys. Res., 118, 3260–3277, doi:10.1002/jgrc.20244, 2013.

Vass, I.: Role of charge recombination processes in photodamage and photoprotection of the photosystem II complex, Physiol. Plant., 142, 6–16, doi:10.1111/j.1399-3054.2011.01454.x, 2011.

25 Vassiliev, I. R., Kolber, Z., Wyman, K. D., Mauzerall, D., Shukla, V. K., and Falkowski, P. G.: Effects of iron limitation on photosystem II composition and light utilization in *Dunaliella tertiolecta*, Plant Physiol., 109, 963–972, doi:10.1104/pp.109.3.963, 1995.

30 Webb, W. L., Newton, M., and Starr, D.: Carbon dioxide exchange of *Alnus rubra*. A mathematical model, Oecologia, 17, 281–291, 1974.

Welschmeyer, N. A.: Fluorometric analysis of chlorophyll *a* in the presence of chlorophyll *b* and pheopigments, Limnol. Oceanogr., 39, 1985–1992, 1994.

BGD

12, 16803–16845, 2015

Diurnal variation in the coupling of photosynthetic electron transport

N. Schuback et al.

Title Page

Abstract

Introduction

Conclusions

References

Tables

Figures

◀

▶

◀

▶

Back

Close

Full Screen / Esc

Printer-friendly Version

Interactive Discussion



- Williams, P. J. le B., Thomas, D. N., and Reynolds, C. S.: Phytoplankton Productivity: Carbon Assimilation in Marine and Freshwater Ecosystems, John Wiley and Sons, New York, 2008.
- Yruela, I.: Transition metals in plant photosynthesis, *Met. Integr. Biometal Sci.*, 5, 1090–1109, doi:10.1039/c3mt00086a, 2013.
- 5 Zehr, J. P. and Kudela, R. M.: Photosynthesis in the Open Ocean, *Science*, 326, 945–946, doi:10.1126/science.1181277, 2009.
- Zhao, Y. and Quigg, A.: Study of photosynthetic productivity in the Northern Gulf of Mexico: importance of diel cycles and light penetration, *Cont. Shelf Res.*, 102, 33–46, doi:10.1016/j.csr.2015.04.014, 2015.

Diurnal variation in the coupling of photosynthetic electron transport

N. Schuback et al.

Title Page

Abstract

Introduction

Conclusions

References

Tables

Figures



Back

Close

Full Screen / Esc

Printer-friendly Version

Interactive Discussion



BGD

12, 16803–16845, 2015

Diurnal variation in the coupling of photosynthetic electron transport

N. Schuback et al.

Table 1. Parameters measures at each time-point during the diurnal experiment.

Time Point	1	2	3	4	5	6	7	8
Local time	3:00	6:00	9:00	12:00	15:00	18:00	21:00	0:00
[chl <i>a</i>]	x	x	x	x	x	x	x	x
HPLC	x		x		x		x	
Absorption Spectra	x	x	x	x	x	x	x	x
FRRF measurements	x	x	x	x	x	x	x	x
C-fixation	x	x	x	x	x	x	x	x

Title Page

Abstract

Introduction

Conclusions

References

Tables

Figures



Back

Close

Full Screen / Esc

Printer-friendly Version

Interactive Discussion



Diurnal variation in the coupling of photosynthetic electron transport

N. Schuback et al.

Title Page

Abstract

Introduction

Conclusions

References

Tables

Figures

◀

▶

◀

▶

Back

Close

Full Screen / Esc

Printer-friendly Version

Interactive Discussion



Table 2. Phytoplankton pigments used for the derivation of diagnostic pigment ratios. Pigments identified from HPLC analysis were chlorophyll c_3 (Chl c_3), chlorophyll c_1c_2 (Chl c_1c_2), 19′butanoyloxyfucoxanthin (19′ButFuc), fucoxanthin (Fuco), 19′hexanoyloxyfucoxanthin (19′HexFuc), 9′cis-neoxanthin (Neo), prasinoxanthin (Prasino), violaxanthin (Viola), diadinoxanthin (Dd), alloxanthin (Allox), diatoxanthin (Dt), lutein, zeaxanthin (Zea), chlorophyll b (Chl b), chlorophyll a Allomer (Chl a allomer), chlorophyll a + divinyl chlorophyll a (Chl a), chlorophyll a' (Chl a prime), α carotene (α carot), β carotene (β carot).

Pigment group	Pigments
Photoprotective carotenoids (PPC)	Neo + Viola + Dd + Allox + Dt + Lutein + Zea + β carot
Photosynthetic carotenoids (PSC)	19′ButFuc + Fuco + 19′HexFuc + Prasino + α carot
Total chlorophyll (Tchl)	Chl c_3 + Chl c_1c_2 + Chl b + Chl a allomer + Chl a + Chl a prime
Total pigment (TPig)	PPC + PSC + Tchl

Diurnal variation in the coupling of photosynthetic electron transport

N. Schuback et al.

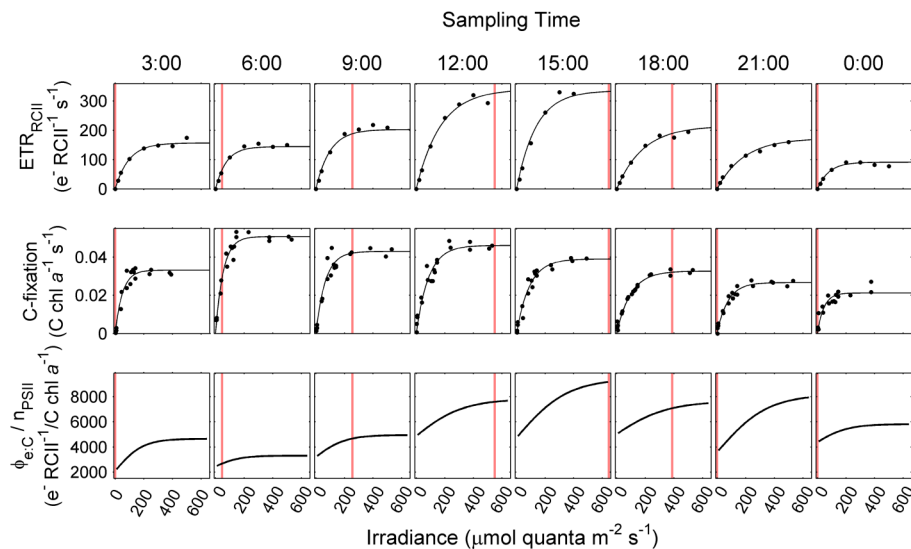


Figure 1. Diurnal variation in rates and light dependency of ETR_{RCII} , carbon fixation and the derived conversion factor $\Phi_{\text{e:c}}/n_{\text{PSII}}$. P vs. E curves of ETR_{RCII} ($\text{mol e}^- \text{mol RCI}^{-1} \text{s}^{-1}$) and carbon fixation ($\text{mol C mol chl a}^{-1} \text{s}^{-1}$) were measured at 3 h intervals over a 24 h diurnal cycle. Data were fit to the exponential model of Webb et al. (1974). The conversion factor $\Phi_{\text{e:c}}/n_{\text{PSII}}$ ($\text{mol e}^- \text{mol RCI}^{-1} / \text{mol C mol chl a}^{-1}$), and its light dependency, were derived as the quotient of corresponding values of ETR_{RCII} and carbon fixation. The vertical line on plots corresponds to in situ PAR values at 5 m depth during sampling for each time-point.

Title Page

Abstract

Introduction

Conclusions

References

Tables

Figures

◀

▶

◀

▶

Back

Close

Full Screen / Esc

Printer-friendly Version

Interactive Discussion



Diurnal variation in the coupling of photosynthetic electron transport

N. Schuback et al.

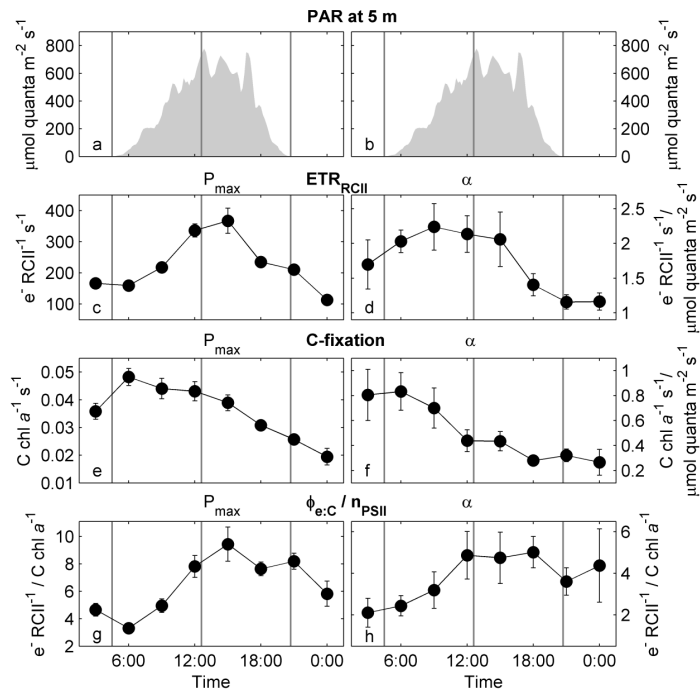


Figure 2. Diurnal changes in P_{\max} (**b–d**) and α (**e–g**) of carbon fixation, ETR_{RCII} and the derived conversion factor $\Phi_{\text{e:C}}/\eta_{\text{PSII}}$. The conversion factor $\Phi_{\text{e:C}}/\eta_{\text{PSII}}$ at light saturation is derived from the values in (**c**) and (**e**). Similarly, the conversion factor $\Phi_{\text{e:C}}/\eta_{\text{PSII}}$ under light limiting conditions is derived from values in (**d**) and (**f**). The error in (**b**), (**c**), (**e**), and (**f**) is the 95 % confidence interval of the parameter derived from the fit to data shown in Fig. 1, and the error in (**d**) and (**g**) is the propagated error for (**b**)/(**c**) and (**e**)/(**f**), respectively. PAR at 5 m depth is shown in (**a**) and (**b**). The vertical gray lines in all plots mark sunrise, solar noon and sunset.

[Title Page](#)
[Abstract](#)
[Introduction](#)
[Conclusions](#)
[References](#)
[Tables](#)
[Figures](#)
[Back](#)
[Close](#)
[Full Screen / Esc](#)
[Printer-friendly Version](#)
[Interactive Discussion](#)

Diurnal variation in the coupling of photosynthetic electron transport

N. Schuback et al.

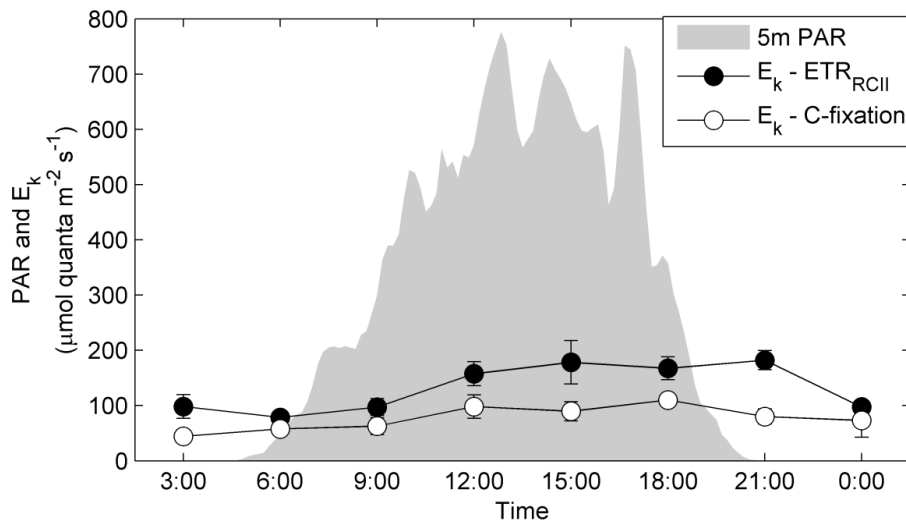


Figure 3. Diurnal variation in the light saturation point E_k of ETR_{RCII} and carbon fixation in relation to in situ PAR at 5 m depth. E_k was derived as P_{max}/α from P vs. E curves of each rate, measured at each TP and error bars are the propagated error.

Title Page

Abstract

Introduction

Conclusions

References

Tables

Figures

◀

▶

◀

▶

Back

Close

Full Screen / Esc

Printer-friendly Version

Interactive Discussion



Diurnal variation in the coupling of photosynthetic electron transport

N. Schuback et al.

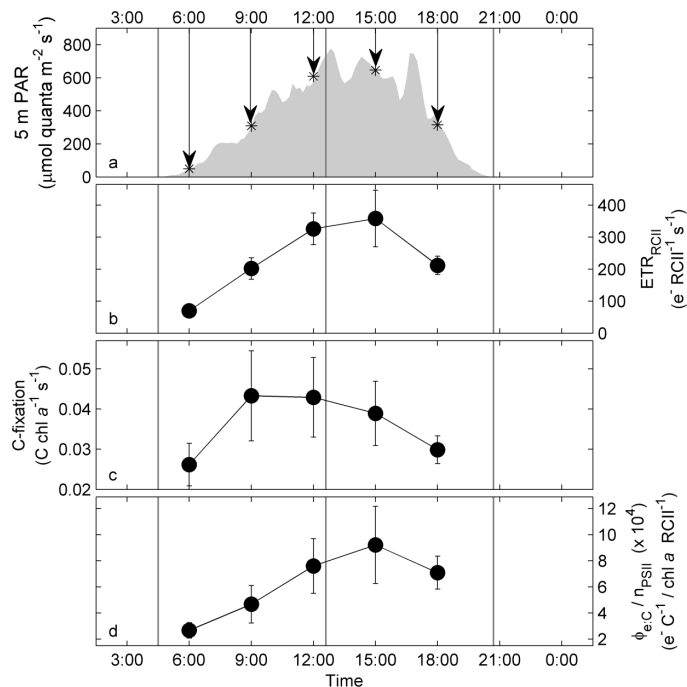


Figure 4. Diurnal changes in ETR_{RCII} , carbon fixation and $\Phi_{e:C}/n_{PSII}$ derived for in situ light intensities at 5 m depth. Diurnal changes in irradiance at 5 m depth (**a**), with arrows indicating the PAR value used to derive rates in (**b**) and (**c**). Realized rates of ETR_{RCII} (**b**) and carbon fixation (**c**) at each time-point were derived from the P vs. E relationship established in Fig. 1. The error in (**b**) and (**c**) is the propagated 95 % confidence interval of the parameter P vs. E fit parameters, and the error in (**d**) is the propagated error from (**b**)/(**c**). The vertical gray lines in all plots mark sunrise, solar noon and sunset.

Title Page

Abstract

Introduction

Conclusions

References

Tables

Figures

◀

▶

◀

▶

Back

Close

Full Screen / Esc

Printer-friendly Version

Interactive Discussion



Diurnal variation in the coupling of photosynthetic electron transport

N. Schuback et al.

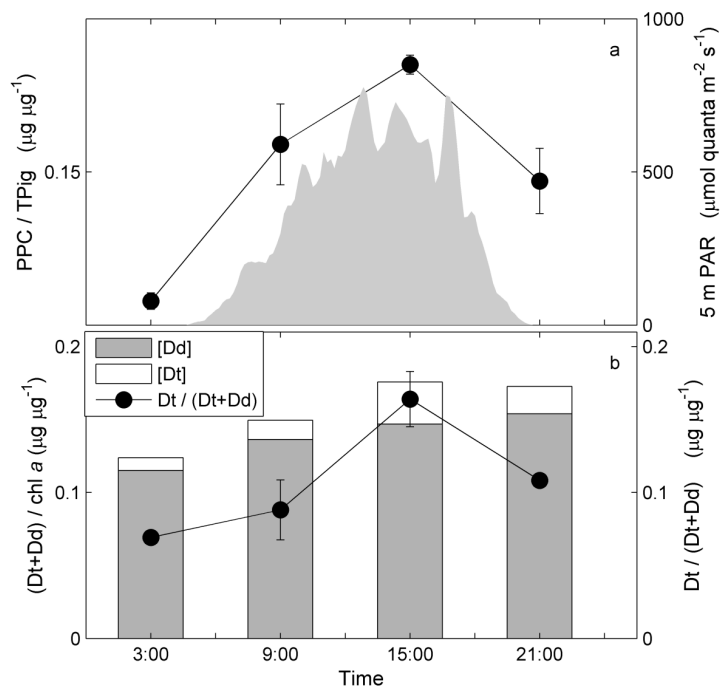


Figure 5. Diurnal changes in pigment ratios. **(a)** shows changes in the abundance of all photoprotective pigment (PPC), relative to the total pigment present (TPig) at each time-point. **(b)** shows relative changes in the abundance of the chromophyte xanthophyll cycling pigments Dd and Dt, normalized to [chl a]. Changes in the de-epoxidation state ratio (DES ratio = $Dt/(Dt + Dd)$), also shown in **(b)**, indicate the extent of active photo-protective energy dissipation through xanthophyll cycling in the pigment antenna. Error bars are the range of values from two replicate samples taken at each time-point. See Table 2 for a definition of pigment groups used to derive these ratios.

Diurnal variation in the coupling of photosynthetic electron transport

N. Schuback et al.

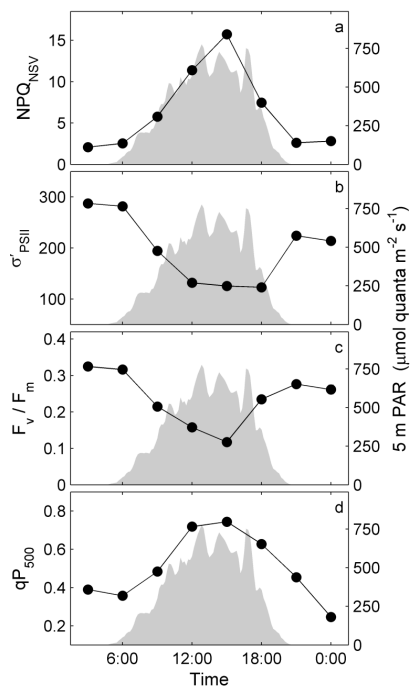


Figure 6. Diurnal changes in PSII photophysiological parameters derived from FRRF measurements. **(a)** shows the normalized Stern–Volmer quenching, NPQ_{NSV} , derived as F'_0/F'_V (McKew et al., 2013) and **(b)** shows the functional absorption cross section, σ'_{PSII} , as estimated for in situ light availability at each TP. Values in **(a)** and **(c)** were calculated by extrapolating between values derived for each light step of the FRRF steady state light curves. **(c)** shows F_v/F_m in the dark-regulated state at each TP, and **(d)** shows estimates of photochemical quenching ($qP = F'_q/F'_V$), indicating the fraction of open RCII (primary stable electron acceptor Q_A oxidized) at a reference irradiance level of $500 \mu\text{mol quanta m}^{-2} \text{s}^{-1}$ (qP_{500}).

Title Page

Abstract

Introduction

Conclusions

References

Tables

Figures

◀

▶

◀

▶

Back

Close

Full Screen / Esc

Printer-friendly Version

Interactive Discussion



Diurnal variation in the coupling of photosynthetic electron transport

N. Schuback et al.

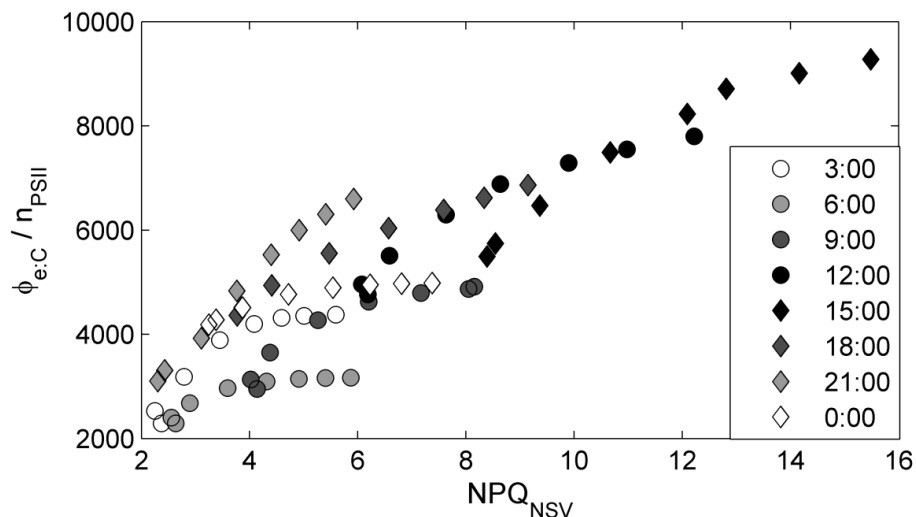


Figure 7. Correlation between the conversion factor $\Phi_{e:C}/\eta_{PSII}$ and the expression of NPQ_{NSV} . NPQ_{NSV} was derived as F'_o/F'_v (McKew et al., 2013), for each step of the FRRF light curve at each TP. Values of $\Phi_{e:C}/\eta_{PSII}$ corresponding to the same light intensities were derived by extrapolation along the carbon fixation and ETR_{RCII} based P vs. E curves. Values of TPs before solar noon are circles, and darkness of symbols increases towards noon. Values for TPs after noon are diamonds, and darkness of symbols decreases towards night.

Title Page

Abstract

Introduction

Conclusions

References

Tables

Figures

⏪

⏩

◀

▶

Back

Close

Full Screen / Esc

Printer-friendly Version

Interactive Discussion

